ized by host cells packed full of fluorescent parasites unable to egress efficiently. These grossly swollen cells often detached from the monolayer and could be found floating in the culture medium giving the appearance of a hot air balloon convention.

Fibroblast cell lines derived from CAPNS1 KO mouse embryos lack both calpain-1 and -2 activity (*30*), and infection of these cells with *T. gondii* produced the same swollen cell phenotype observed in CAPNS1 knock-down experiments (Fig. 3C). Transgenic expression of CAPNS1 in the KO mutants restores calpain-1 and -2 activity (*30*) and also complemented the *T. gondii* egress defect. Parasite tachyzoites were readily able to invade (Fig. 3D) and replicate (Fig. 3E) in WT, CAPNS1 KOs, and CAPNS1-complemented fibroblasts, demonstrating that the impact of host cell calpains on *T. gondii* infection is specific to egress. Plaque assays showed a ~13-fold reduction in plaque size for *T. gondii* in CAPNS1 mutants versus parental MEF cells or CAPNS1-complemented KOs (Fig. 3, F and G). In contrast to *P. falciparum*, which rarely emerge from calpain-depleted erythrocytes (Fig. 2), some *T. gondii* parasites did eventually manage to escape from calpain-deficient fibroblasts, yielding a small plaque phenotype.

In summary, in addition to the many roles that parasite-encoded cysteine proteases play in the biology of infection and pathogenesis (*25*), the apicomplexans *Plasmodium falciparum* and *Toxoplasma gondii* both exploit host cell calpains to facilitate escape from the intracellular parasitophorous vacuole and/or host plasma membrane. The precise mechanism of calpain-mediated parasite egress is unknown, but calpains play a role in remodeling of the cytoskeleton and plasma membrane during the migration of mammalian cells (*31*), and activated calpain-1 can degrade erythrocyte cytoskeletal proteins in vitro and during *P. falciparum* infection in vivo (fig. S4). The calcium responsible for calpain activation during parasite infection may be supplied through the action of a parasite-encoded perforin recently implicated in *T. gondii* egress (*32*). The parasitophorous vacuole was labeled by the calcium-specific dye Fluo-4-AM during late schizogony, and depletion of internal calcium with the membrane-permeant chelator EGTA-AM blocked parasite egress, whereas removal of calcium from the culture medium did not (fig. S5). We suggest a model in which a calcium signal triggered late during parasite infection activates host cell calpain, which relocalizes to the host plasma membrane, cleaving cytoskeletal proteins to facilitate parasite egress (fig. S6). Because parasites that fail to escape from their host cells are unable to proliferate, this suggests an intriguing strategy for anti-parasitic therapeutics.

References and Notes

1. M. Nishi, K. Hu, J. M. Murray, D. S. Roos, *J. Cell Sci.* **121**, 1559 (2008).
2. K. Hu *et al.*, *Mol. Biol. Cell* **13**, 593 (2002).
3. S. Glushakova, D. Yin, T. Li, J. Zimmerberg, *Curr. Biol.* **15**, 1645 (2005).
4. B. L. Salmon, A. Oksman, D. E. Goldberg, *Proc. Natl. Acad. Sci. U.S.A.* **98**, 271 (2001).
5. M. W. Black, G. Arrizabalaga, J. C. Boothroyd, *Mol. Cell. Biol.* **20**, 9399 (2000).
6. K. Nagamune *et al.*, *Nature* **451**, 207 (2008).
7. T. Hadley, M. Aikawa, L. H. Miller, *Exp. Parasitol.* **55**, 306 (1983).
8. M. E. Wickham, J. G. Culvenor, A. F. Cowman, *J. Biol. Chem.* **278**, 37658 (2003).
9. S. Arastu-Kapur *et al.*, *Nat. Chem. Biol.* **4**, 203 (2008).
10. S. Yeoh *et al.*, *Cell* **131**, 1072 (2007).
11. D. C. Greenbaum *et al.*, *Science* **298**, 2002 (2002).
12. S. Glushakova, J. Mazar, M. F. Hohmann-Marriott, E. Hama, J. Zimmerberg, *Cell. Microbiol.* **11**, 95 (2009).
13. Materials and methods are available as supporting material on *Science* Online.
14. I. Russo, A. Oksman, B. Vaupel, D. E. Goldberg, *Proc. Natl. Acad. Sci. U.S.A.* **106**, 1554 (2009).
15. E. M. Pasini *et al.*, *Blood* **108**, 791 (2006).
16. D. E. Croall, K. Ersfeld, *Genome Biol.* **8**, 218 (2007).
17. D. E. Goll, V. F. Thompson, H. Li, W. Wei, J. Cong, *Physiol. Rev.* **83**, 731 (2003).
18. S. C. Murphy *et al.*, *PLoS Med.* **3**, e528 (2006).
19. R. A. Hanna, R. L. Campbell, P. L. Davies, *Nature* **456**, 409 (2008).
20. T. Moldoveanu, K. Gehring, D. R. Green, *Nature* **456**, 404 (2008).
21. S. Gil-Parrado *et al.*, *Biol. Chem.* **384**, 395 (2003).
22. A. E. Bianco, F. L. Battye, G. V. Brown, *Exp. Parasitol.* **62**, 275 (1986).
23. M. Hanspal, V. K. Goel, S. S. Oh, A. H. Chishti, *Mol. Biochem. Parasitol.* **122**, 227 (2002).
24. L. Weiss, J. Johnson, W. Weidanz, *Am. J. Trop. Med. Hyg.* **41**, 135 (1989).
25. P. J. Rosenthal, *Int. J. Parasitol.* **34**, 1489 (2004).
26. P. Dutt *et al.*, *BMC Dev. Biol.* **6**, 3 (2006).
27. J. S. Arthur, J. S. Elce, C. Hegadorn, K. Williams, P. A. Greer, *Mol. Cell. Biol.* **20**, 4474 (2000).
28. D. S. Roos, R. G. Donald, N. S. Morrissette, A. L. Moulton, *Methods Cell Biol.* **45**, 27 (1994).
29. K. A. Joiner, D. S. Roos, *J. Cell Biol.* **157**, 557 (2002).
30. N. Dourdin *et al.*, *J. Biol. Chem.* **276**, 48382 (2001).
31. A. Huttenlocher *et al.*, *J. Biol. Chem.* **272**, 32719 (1997).
32. B. F. C. Kafsack *et al.*, *Science* **323**, 530 (2009); published online 18 December 2008 (10.1126/science.1165740).
33. We thank R. W. Doms, M. Marti, and M. Klemba for critical discussions; the Penn Proteomics Core for mass spectrometry; and M. A. Lampson for help with imaging. *P. falciparum* expressing GFP were provided by O. S. Harb. P.H.D. and D.P.B. are funded by National Research Service Awards, and D.S.R. is an Ellison Medical Foundation Senior Scholar in Global Infectious Disease, supported by grants from NIH. D.C.G. was supported by the Ritter Foundation, the Penn Genome Frontiers Institute, and the Penn Institute for Translational Medicine and Therapeutics.

Supporting Online Material

www.sciencemag.org/cgi/content/full/1171085/DC1
Materials and Methods
Figs. S1 to S6
Table S1
References

20 January 2009; accepted 10 March 2009
Published online 2 April 2009;
10.1126/science.1171085
Include this information when citing this paper.

Human Induced Pluripotent Stem Cells Free of Vector and Transgene Sequences

Junying Yu,[1,2,3]* Kejin Hu,[3] Kim Smuga-Otto,[1,2,3] Shulan Tian,[1,2] Ron Stewart,[1,2] Igor I. Slukvin,[3,4] James A. Thomson[1,2,3,5]*

Reprogramming differentiated human cells to induced pluripotent stem (iPS) cells has applications in basic biology, drug development, and transplantation. Human iPS cell derivation previously required vectors that integrate into the genome, which can create mutations and limit the utility of the cells in both research and clinical applications. We describe the derivation of human iPS cells with the use of nonintegrating episomal vectors. After removal of the episome, iPS cells completely free of vector and transgene sequences are derived that are similar to human embryonic stem (ES) cells in proliferative and developmental potential. These results demonstrate that reprogramming human somatic cells does not require genomic integration or the continued presence of exogenous reprogramming factors and removes one obstacle to the clinical application of human iPS cells.

The proliferative and developmental potential of both human embryonic stem (ES) cells and human induced pluripotent stem (iPS) cells offers unprecedented access to the differentiated cells that make up the human body (*1*–*3*). In addition, iPS cells can be derived with a specific desired genetic background, including patient-specific iPS cells for disease models and for transplantation therapies, without the problems associated with immune rejection. Reprogramming of both mouse and human somatic cells into iPS cells has been achieved by expressing combinations of factors such as *OCT4*, *SOX2*, c-*Myc*, *KLF4, NANOG*, and *LIN28* (*2*–*4*). Initial methods used to derive human iPS cells used viral vectors, in which both the vector backbone and transgenes are permanently integrated into the genome (*2*, *3*). Such vectors can produce insertional mutations that interfere with the normal function of iPS cell derivatives, and residual transgene expression can influence differentiation into specific lineages (*2*), or even result in tumorigenesis (*5*). Vector integration–free mouse iPS cells have been derived from

liver cells with adenoviral vectors (*6*) and from embryonic fibroblasts with repeated plasmid transfections (*7*), but the low frequencies obtained make it unclear how practical these approaches will be for human cells, which generally require longer exposure to reprogramming factors (*2*, *3*).

While this manuscript was in review, two alternative approaches were described to remove transgenes from mouse or human iPS cells. In one approach, Cre/LoxP recombination was used to excise integrated transgenes (*8*, *9*). This approach successfully removes transgene sequences, but leaves behind residual vector sequences, which can still create insertional mutations. A second approach used seamless excision of piggyBac transposons to produce vector- and transgene-free mouse iPS cells (*10*). Although a promising approach, vector removal from human iPS cells produced by this method has not yet been reported, and removing multiple transposons is labor intensive. Here, we report that human iPS cells completely free of vector and transgene sequences can be derived from fibroblasts by a single transfection with oriP/EBNA1 (Epstein-Barr nuclear antigen-1)–based episomal vectors.

Derived from the Epstein-Barr virus, oriP/EBNA1 vectors are well suited for introducing reprogramming factors into human somatic cells, as these plasmids can be transfected without the need for viral packaging and can be subsequently removed from cells by culturing in the absence of drug selection. The stable extrachromosomal replication of oriP/EBNA1 vectors in mammalian cells requires only a cis-acting oriP element (*11*) and a trans-acting EBNA1 gene (*12*). The oriP/EBNA1 vectors replicate only once per cell cycle, and with drug selection can be established as stable episomes in about 1% of the initial transfected cells (*13*, *14*). If drug selection is subsequently removed, the episomes are lost at ~5% per cell generation owing to defects in plasmid synthesis and partitioning; thus, cells devoid of plasmids can be easily isolated (*15*).

OCT4, *SOX2*, *NANOG*, and *LIN28* are sufficient to reprogram human embryonic, neonatal, and adult fibroblasts to iPS cells (*2*, *16*), but the reprogramming efficiency is low (<0.01% for newborn foreskin fibroblasts) (*2*). Such low efficiency makes it difficult to reprogram with oriP/EBNA1-based vectors because the stable transfection efficiency is almost two orders of magnitude less than that of our lentiviral vectors (*2*). Thus, we first improved reprogramming efficiency with lentiviral vectors. By testing different linkers to coexpress *OCT4* and *SOX2*, we found that the internal ribosome entry site 2 (IRES2) supported higher reprogramming efficiency (fig. S1, A and B). Because linkers have less effect on reprogramming efficiency when used to coexpress *NANOG* and *LIN28* (fig. S1B), IRES2 was chosen to coexpress reprogramming factors. Using IRES2-mediated expression of OCT4, SOX2, NANOG, and LIN28, we improved the reprogramming efficiency for human foreskin fibroblasts by about 10-fold (~0.1%) over what we had previously reported (fig. S1C). The addition of c-Myc and KLF4 further improved the reprogramming efficiency to more than 1%, the highest efficiencies we have achieved for these cells (fig. S1C) (*17*). Thus, we cloned all six reprogramming factors (*OCT4*, *SOX2*, *NANOG*, *LIN28*, c-*Myc*, and *KLF4*) into an oriP/EBNA1 vector using IRES2 for coexpression. Because our previous experience suggested that both the balance between transgenes and their absolute expression levels are critically important to achieving reprogramming, we tested different transgene arrangements to achieve appropriate levels empirically (table S1).

Initial tests with the six reprogramming genes in the episomal vectors failed to yield human iPS cell colonies (table S2). With this combination of genes, substantial cell death was observed during the first week after transfection, possibly

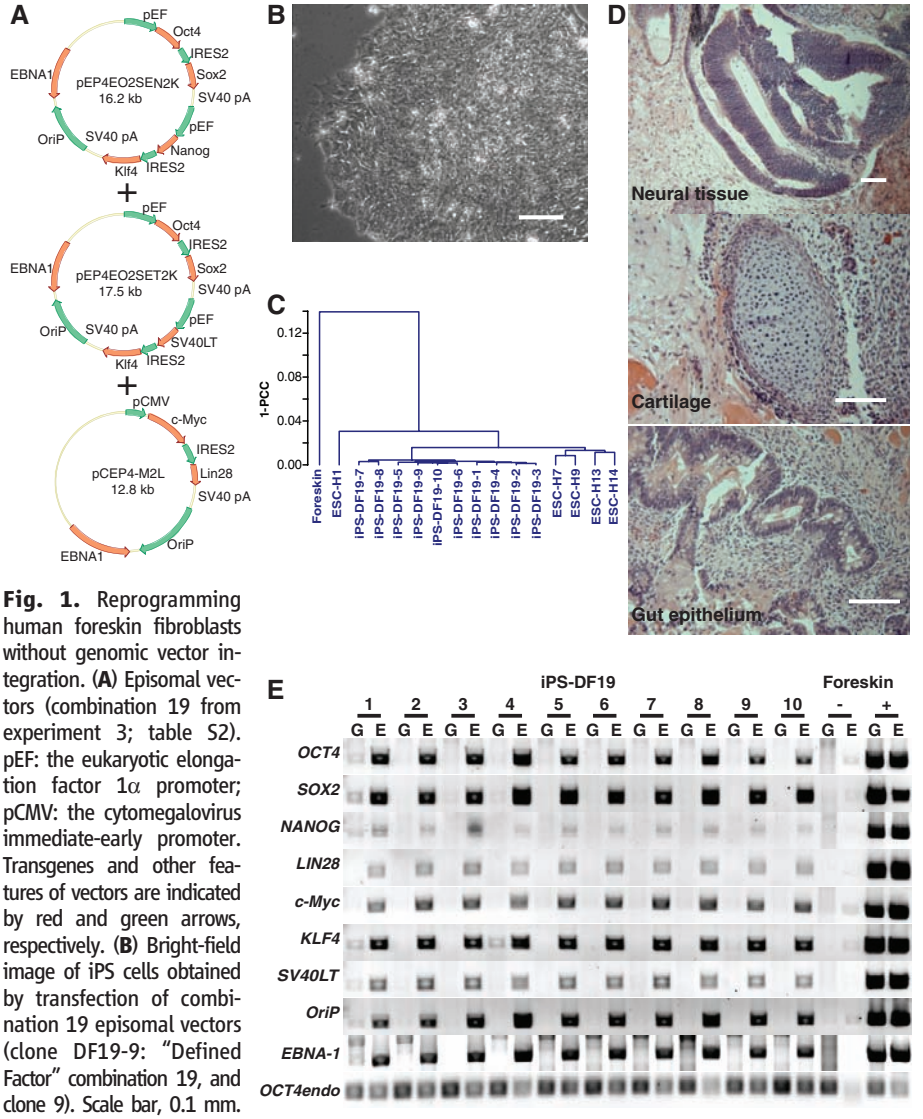

Fig. 1. Reprogramming human foreskin fibroblasts without genomic vector integration. (**A**) Episomal vectors (combination 19 from experiment 3; table S2). pEF: the eukaryotic elongation factor 1α promoter; pCMV: the cytomegalovirus immediate-early promoter. Transgenes and other features of vectors are indicated by red and green arrows, respectively. (**B**) Bright-field image of iPS cells obtained by transfection of combination 19 episomal vectors (clone DF19-9: "Defined Factor" combination 19, and clone 9). Scale bar, 0.1 mm. (**C**) Pearson correlation analyses of global gene expression (51,337 transcripts) in human fibroblast-derived iPS cell clones (combination 19). 1-PCC: Pearson correlation coefficient. (**D**) Hematoxylin and eosin staining of teratoma sections of iPS cell clone DF19-9 (53 days after injection). Teratomas were obtained from all 10 iPS-DF19 clones. Scale bars, 0.1 mm. (**E**) PCR analysis of episomal DNA in iPS-DF19 clone 1 to 10. G: genomic DNA template; E: episomal DNA template. Genomic and episomal DNA from nontransfected and combination 19 episomal vector-transfected (day 17 after transfection) fibroblasts were used as negative (–) and positive (+) controls, respectively. Thirty-two PCR cycles were used for all primer sets.

[1]Morgridge Institute for Research, Madison, WI 53707–7365, USA. [2]Genome Center of Wisconsin, Madison, WI 53706–1580, USA. [3]Wisconsin National Primate Research Center, University of Wisconsin-Madison, Madison, WI 53715–1299, USA. [4]Department of Pathology and Laboratory Medicine, University of Wisconsin-Madison, Madison, WI 53706, USA. [5]Department of Anatomy, University of Wisconsin-Madison, Madison, WI 53706–1509, USA.

*To whom correspondence should be addressed. E-mail: jyyu2008@gmail.com (J.Y.); thomson@primate.wisc.edu (J.A.T.)

owing to the toxic effects of high c-Myc expression (*18*). To counteract the possible toxic effects of c-Myc expression, we included the SV40 large T gene (*SV40LT*) in some of the combinations (*19*). Three of these combinations, all of which included *OCT4*, *SOX2*, *NANOG*, *LIN28*, c-*Myc*, *KLF4*, and *SV40LT*, were successful in producing iPS cell colonies from human foreskin fibroblasts with oriP/EBNA1-based vectors (Fig. 1A, fig. S2D, and table S2). At least two plasmids in each successful combination express OCT4 and SOX2, consistent with the observation that high expression of these transgenes improves reprogramming. Clones from two of these combinations (19 from experiment 3 and 6 from experiment 4; table S2) were chosen for expansion and analysis. These iPS cell colonies exhibited typical human ES cell morphology (e.g., compact colonies, high nucleus-to-cytoplasm ratios, and prominent nucleoli) (Fig. 1B) and exhibited gene expression profiles that were very similar to those of human ES cell lines, but dissimilar to those of the parental fibroblasts (Fig. 1C and table S3). Similar to human ES cells, when injected into immunocompromised mice, these iPS cells formed teratomas consisting of differentiated derivatives of all three primary

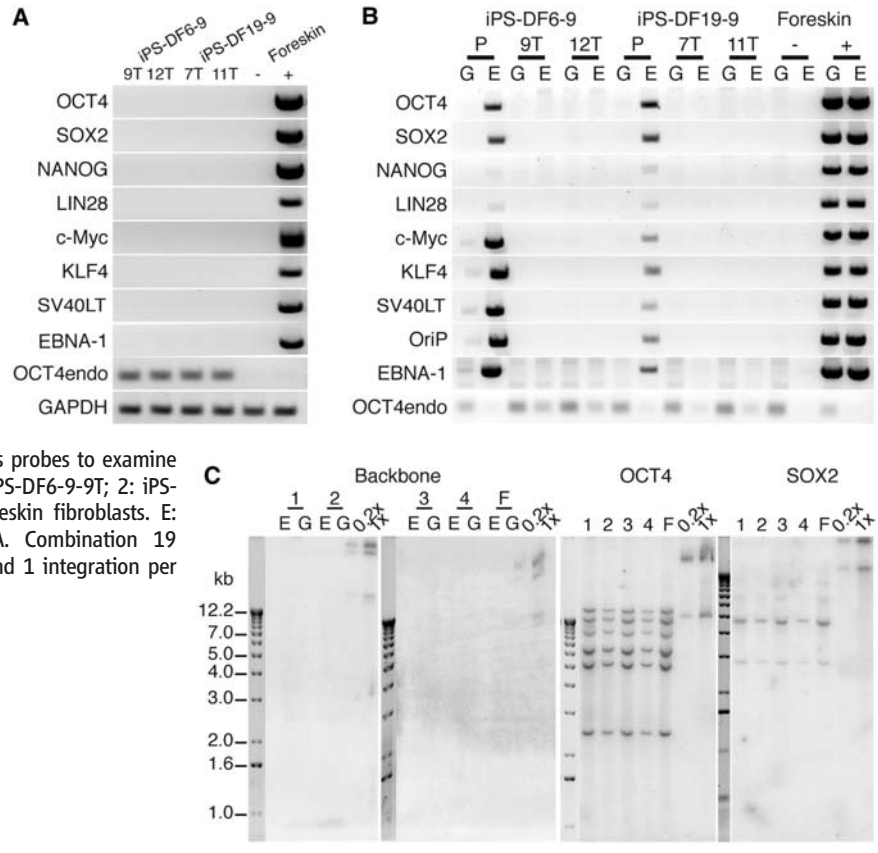

Fig. 2. Human foreskin fibroblast–derived iPS cells free of vectors and transgenes. (**A**) RT-PCR analysis of transgene expression in iPS-DF6-9 subclone 9T and 12T, and iPS-DF-19-9 subclone 7T and 11T. Negative control (–): fibroblasts; positive control (+): fibroblasts transfected with combination 19 episomal vectors (day 4 after transfection). Thirty-two PCR cycles were used for all primer sets. (**B**) PCR analysis of episomal DNA in iPS-DF6-9 (P: parental clone), iPS-DF6-9 subclone 9T and 12T, iPS-DF19-9 (P), and iPS-DF19-9 subclones 7T and 11T. G: genomic DNA template; E: episomal DNA template. Negative (–) and positive (+) controls were the same as in Fig. 1E. Thirty-two PCR cycles were used for all primer sets except *OCT4* endo (28 cycles). (**C**) Southern blot analysis of exogenous DNA in iPS-DF6-9 and iPS-DF-19-9 subclones. The pCEP4 vector was used as a probe to detect the presence of vector backbone, and the open reading frames of *OCT4* and *SOX2* were used as probes to examine both the endogenous gene and possible transgenes. 1: iPS-DF6-9-9T; 2: iPS-DF6-9-12T; 3: iPS-DF19-9-7T; 4: iPS-DF19-9-11T; F: foreskin fibroblasts. E: undigested episomal DNA; G: digested genomic DNA. Combination 19 episomal vector DNA diluted to the equivalents of 0.2 and 1 integration per genome was used as positive controls (0.2× and 1×).

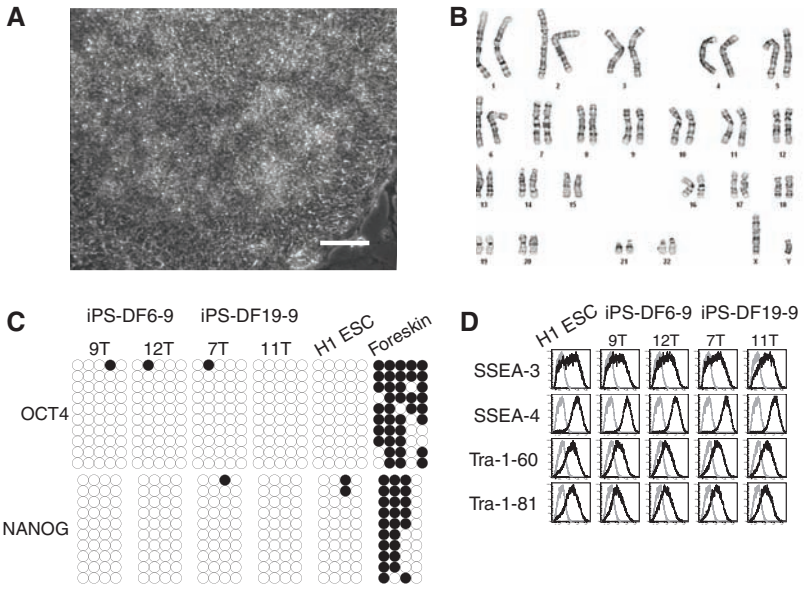

Fig. 3. Characterization of iPS cell subclones. (**A**) Bright-field image of iPS-DF6-9-12T. Scale bar, 0.1 mm. (**B**) G-banding chromosome analysis of iPS-DF6-9-12T. (**C**) Analysis of the methylation status of the *OCT4* and *NANOG* promoters in iPS cell subclones by means of bisulfite sequencing. Open circles indicate unmethylated, and filled circles indicate methylated CpG dinucleotides. (**D**) Flow cytometry expression analysis of human ES cell–specific cell surface markers. Gray line: isotype control; black line: antigen staining.

germ layers (Fig. 1D). Polymerase chain reaction (PCR) analysis failed to detect episomal vector integration in the genome, but did detect their persistence in the episomal fraction (Fig. 1E). The persistence of the episomal vectors suggests that prolonged transgene expression is required for successful reprogramming.

Because oriP/EBNA1 episomal vectors are gradually lost from proliferating cells in the absence of selection, we performed subcloning to derive iPS cell clones that had spontaneously lost the episomal vectors. We chose one iPS cell clone derived with combination 6 (iPS-DF6-9) and another one with combination 19 (iPS-DF19-9), and isolated 12 subclones from each. More than one-third of the subclones lost their episomal vectors (fig. S3A). We expanded two subclones from each vector combination for detailed analysis (iPS-DF6-9 subclone 9T and 12T, iPS-DF19-9 subclone 7T and 11T). Reverse transcription (RT)–PCR analysis with transgene-specific primers failed to detect any residual transgene expression in any of the four iPS cell subclones (Fig. 2A). In contrast to the parental iPS cell clones, PCR analysis demonstrated the absence of the vector and transgene sequences in both the genomic and the episomal fractions of all four iPS cell subclones (Fig. 2B), which was confirmed by Southern blot analysis (Fig. 2C and fig. S3B).

The iPS cell subclones were morphologically similar to human ES cells (Fig. 3A); had normal karyotypes (Fig. 3B); expressed human ES cell–specific cell surface markers (Fig. 3D) and genes (Fig. 4, A and B, fig. S4, and table S4); and differentiated into derivatives of all three germ layers in teratomas (Fig. 4C). Both the *OCT4* promoter and the *NANOG* promoter were demethylated in these iPS cells, similar to human ES cells and in contrast to the parental foreskin fibroblasts (Fig. 3C). As of this writing, combination 19 iPS cells have been in continuous culture for 7 months after the initial fibroblast transfection and have demonstrated no period of replicative crisis. DNA fingerprinting confirmed their origin from foreskin fibroblasts (table S5).

With oriP/EBNA1-based episomal vectors, exogenous DNA is not integrated into the human iPS cell genome, and owing to the gradual loss of cellular episomal vectors in the absence of drug selection, vector- and transgene-free human iPS cells can be isolated through subcloning without further genetic manipulation. Similar to mouse studies based on nonintegrating reprogramming methods (*6*, *7*), the current reprogramming efficiency of human fibroblasts with oriP/EBNA1 vectors is low (about three to six colonies per 10^6 input cells). These frequencies are, however, sufficient to recover iPS cells from a reasonable number of starting cells, and fibroblasts are easy to obtain and culture. Because different cell types have different reprogramming frequencies (*20*), and oriP/EBNA1-based vectors are established as stable episomes at different frequencies in different cell types (*13*), it might be possible to identify another accessible human cell type more easily reprogrammed with these episomal vectors. The addition of chemical compounds that increase reprogramming efficiency might also facilitate reprogramming by these episomal vectors (*21*, *22*).

Given the rapid pace of the iPS cell field, it is likely that reprogramming efficiencies will improve substantially and that it soon will be possible to derive vector- and transgene-free human iPS cells by several alternative methods. However, it will be essential to determine which of these methods most consistently produces iPS cells with the fewest genetic or epigenetic abnormalities, because any abnormalities would affect the application of these cells in basic research, drug development, and transplantation therapies much more than the initial reprogramming frequencies. Substantial challenges also remain in cell-specific differentiation and delivery, but the derivation of vector- and transgene-free human iPS cells is nonetheless an important advance toward the clinical application of these cells.

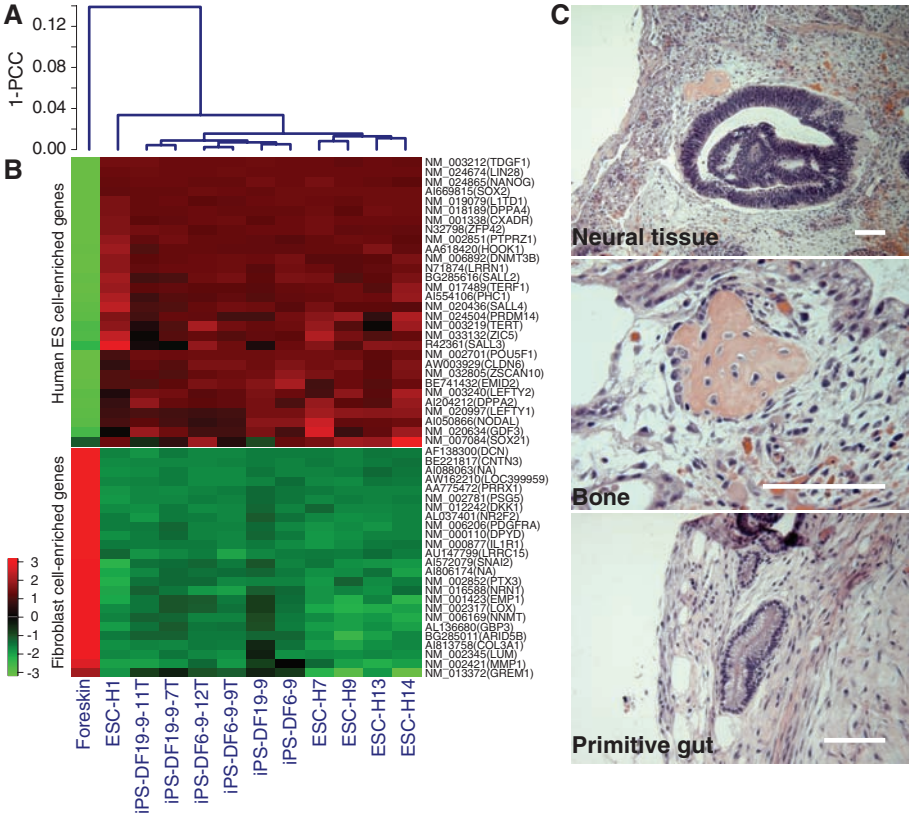

Fig. 4. Characterization of iPS cell subclones. (**A**) Pearson correlation analyses of global gene expression (51,337 transcripts) in iPS cell parental clone DF6-9 and DF19-9; iPS cell subclone DF6-9-9T, DF6-9-12T, DF19-9-7T, and DF19-9-11T; five human ES cell lines; foreskin fibroblasts. 1-PCC: Pearson correlation coefficient. (**B**) Expression of genes that are differentially expressed between human ES cells and foreskin fibroblasts. (Top) Thirty well-known human ES cell–enriched genes; (bottom) top 25 foreskin fibroblast-enriched genes. The color key is shown on the left. (**C**) Hematoxylin and eosin staining of teratoma sections of iPS-DF19-9-11T (7 weeks after injection). Teratomas were obtained from all four iPS cell subclones. Scale bars, 0.1 mm.

References and Notes

1. J. A. Thomson *et al.*, *Science* **282**, 1145 (1998).
2. J. Yu *et al.*, *Science* **318**, 1917 (2007).
3. K. Takahashi *et al.*, *Cell* **131**, 861 (2007).
4. K. Takahashi, S. Yamanaka, *Cell* **126**, 663 (2006).
5. K. Okita, T. Ichisaka, S. Yamanaka, *Nature* **448**, 313 (2007).
6. M. Stadtfeld, M. Nagaya, J. Utikal, G. Weir, K. Hochedlinger, *Science* **322**, 945 (2008).
7. K. Okita, M. Nakagawa, H. Hyenjong, T. Ichisaka, S. Yamanaka, *Science* **322**, 949 (2008).
8. K. Kaji *et al.*, *Nature* **458**, 771 (2009).
9. F. Soldner *et al.*, *Cell* **136**, 964 (2009).
10. K. Woltjen *et al.*, *Nature*, 10.1038/nature07863 (2009).
11. J. Yates, N. Warren, D. Reisman, B. Sugden, *Proc. Natl. Acad. Sci. U.S.A.* **81**, 3806 (1984).
12. J. L. Yates, N. Warren, B. Sugden, *Nature* **313**, 812 (1985).
13. E. R. Leight, B. Sugden, *Mol. Cell. Biol.* **21**, 4149 (2001).
14. J. L. Yates, N. Guan, *J. Virol.* **65**, 483 (1991).
15. A. Nanbo, A. Sugden, B. Sugden, *EMBO J.* **26**, 4252 (2007).
16. A. D. Ebert *et al.*, *Nature* **457**, 277 (2009).
17. J. Liao *et al.*, *Cell Res.* **18**, 600 (2008).
18. G. I. Evan *et al.*, *Cell* **69**, 119 (1992).
19. W. C. Hahn *et al.*, *Nature* **400**, 464 (1999).
20. T. Aasen *et al.*, *Nat. Biotechnol.* **26**, 1276 (2008).
21. Y. Shi *et al.*, *Cell Stem Cell* **3**, 568 (2008).
22. D. Huangfu *et al.*, *Nat. Biotechnol.* **26**, 795 (2008).

23. Funding was provided by the Charlotte Geyer Foundation and NIH (grants P51 RR000167 and P01 GM081629). We thank A. Griep, P. Powers, B. Sugden, M. Probasco, A. Elwell, C. Glennon, V. Ruotti, and D. J. Faupel for assistance and advice. The authors declare competing financial interests: J.A.T. is a founder, stock owner,

consultant, and board member of Cellular Dynamics International (CDI). He also serves as a scientific adviser to and has financial interests in Tactics II Stem Cell Ventures. I.I.S. is a founder, stock owner, and consultant for CDI. The authors are filing a patent based on the results reported in this paper. Combination 6 and 19 episomal vectors are deposited in Addgene (Cambridge, MA), and vector-free human iPS cell subclones are deposited in the WiCell International Stem Cell (WISC) Bank (Madison, WI). Microarray data are deposited in the Gene Expression Omnibus (GEO) database (accession number GSE15148).

Supporting Online Material
www.sciencemag.org/cgi/content/full/1172482/DC1
Materials and Methods
Figs. S1 to S4
Tables S1 to S8
References

18 February 2009; accepted 17 March 2009
Published online 26 March 2009;
10.1126/science.1172482
Include this information when citing this paper.

Benzothiazinones Kill *Mycobacterium tuberculosis* by Blocking Arabinan Synthesis

Vadim Makarov,[1,2]* Giulia Manina,[1,3]* Katarina Mikusova,[1,4]* Ute Möllmann,[1,5]* Olga Ryabova,[1,2] Brigitte Saint-Joanis,[1,6] Neeraj Dhar,[7] Maria Rosalia Pasca,[1,3] Silvia Buroni,[1,3] Anna Paola Lucarelli,[1,3] Anna Milano,[1,3] Edda De Rossi,[1,3] Martina Belanova,[1,4] Adela Bobovska,[1,4] Petronela Dianiskova,[1,4] Jana Kordulakova,[1,4] Claudia Sala,[1,7] Elizabeth Fullam,[1,7] Patricia Schneider,[1,7] John D. McKinney,[7] Priscille Brodin,[8] Thierry Christophe,[8] Simon Waddell,[1,9] Philip Butcher,[1,9] Jakob Albrethsen,[1,10] Ida Rosenkrands,[1,10] Roland Brosch,[1,6] Vrinda Nandi,[1,11] Sowmya Bharath,[1,11] Sheshagiri Gaonkar,[1,11] Radha K. Shandil,[1,11] Venkataraman Balasubramanian,[1,11] Tanjore Balganesh,[1,11] Sandeep Tyagi,[12] Jacques Grosset,[12] Giovanna Riccardi,[1,3] Stewart T. Cole[1,7]†

New drugs are required to counter the tuberculosis (TB) pandemic. Here, we describe the synthesis and characterization of 1,3-benzothiazin-4-ones (BTZs), a new class of antimycobacterial agents that kill *Mycobacterium tuberculosis* in vitro, ex vivo, and in mouse models of TB. Using genetics and biochemistry, we identified the enzyme decaprenylphosphoryl-β-D-ribose 2′-epimerase as a major BTZ target. Inhibition of this enzymatic activity abolishes the formation of decaprenylphosphoryl arabinose, a key precursor that is required for the synthesis of the cell-wall arabinans, thus provoking cell lysis and bacterial death. The most advanced compound, BTZ043, is a candidate for inclusion in combination therapies for both drug-sensitive and extensively drug-resistant TB.

The loss of human lives to tuberculosis (TB) continues essentially unabated as a result of poverty, synergy with the HIV/AIDS pandemic, and the emergence of multi- drug- and extensively drug-resistant strains of *Mycobacterium tuberculosis* (*1*–*3*). Despite some recent successes, such as the discovery of the diarylquinoline drug TMC207 (*4*) and the promise of the bicyclic nitroimidazole compounds (*5*–*8*), and because of the high attrition rate in drug development (*9*), much greater effort is required to find better drugs in order to meet the desired goals of killing persistent tubercle bacilli and reducing TB treatment duration from 6 to less than 3 months (*10*, *11*).

A series of sulfur-containing heterocycles was synthesized and tested for antibacterial and antifungal activity (*12*, *13*). Among their derivatives, compounds belonging to the nitrobenzothiazinone (BTZ) class showed particular promise in terms of their potency and specificity for mycobacteria. One of them, 2-[2-methyl-1,4-dioxa-8-azaspiro[4.5]dec-8-yl]-8-nitro-6-(trifluoromethyl)-4*H*-1,3-benzothiazin-4-one (BTZ038), was selected for further studies. This compound (series number 10526038; $C_{17}H_{16}F_3N_3O_5S$, with a molecular weight of 431.4; log$P$ = 2.84) (Fig. 1A) was synthesized in seven steps with a yield of 36%. Structure activity relationship work showed that the sulfur atom and the nitro group at positions 1 and 8, respectively, were critical for activity. BTZ038 has a single chiral center, and both enantiomers, BTZ043 (*S*) and BTZ044 (*R*), were found to be equipotent in vitro. Because early metabolic studies with bacteria or mice indicated that the nitro group could be reduced to an amino group, and because many TB drugs are prodrugs that require activation by *M. tuberculosis* (*14*), the *S* and *R* enantiomers of the amino derivatives and the likely hydroxylamine intermediate were synthesized and tested for antimycobacterial activity in vitro (table S1). The amino (BTZ045, *S* and *R*) and hydroxylamine (BTZ046) derivatives were substantially less active (500- to 5000-fold).

The minimal inhibitory concentrations (MICs) of a variety of BTZs against different mycobacteria were very low, ranging from ~0.1 to 80 ng/ml for fast growers and from 1 to 30 ng/ml for members of the *M. tuberculosis* complex (*13*). The MIC of BTZ043 against *M. tuberculosis* H37Rv and *Mycobacterium smegmatis* were 1 ng/ml (2.3 nM) and 4 ng/ml (9.2 nM), respectively (Table 1), which compares favorably with those of the existing TB drugs isoniazid (INH) (0.02 to 0.2 μg/ml) and ethambutol (EMB) (1 to 5 μg/ml) (*14*). From structure activity relationship studies, >30 different BTZ derivatives showed MICs of <50 ng/ml against tubercle

Table 1. MIC of BTZ043 against three different mycobacterial species and their resistant mutants.

Strain	MIC (ng/ml)	Codon	Amino acid
M. smegmatis mc^{2}155	4	TGC	Cysteine
M. smegmatis MN47	4000	GGC	Glycine
M. smegmatis MN84	>16,000	TCC	Serine
M. bovis BCG	2	TGC	Cysteine
M. bovis BCG BN2	>16,000	TCC	Serine
M. tuberculosis H37Rv	1	TGC	Cysteine
M. tuberculosis NTB9	250	GGC	Glycine
M. tuberculosis NTB1	10,000	TCC	Serine

[1]New Medicines for Tuberculosis (NM4TB) Consortium (www.nm4tb.org). [2]A. N. Bakh Institute of Biochemistry, Russian Academy of Science, 119071 Moscow, Russia. [3]Dipartimento di Genetica e Microbiologia, Università degli Studi di Pavia, via Ferrata, 1, 27100 Pavia, Italy. [4]Department of Biochemistry, Faculty of Natural Sciences, Comenius University, Mlynska dolina, 84215 Bratislava, Slovakia. [5]Department of Molecular and Applied Microbiology, Leibniz Institute for Natural Product Research and Infection Biology–Hans Knoell Institute, Beutenbergstrasse 11a, D-07745 Jena, Germany. [6]Institut Pasteur, Integrated Mycobacterial Pathogenomics, 25-28, Rue du Docteur Roux, 75724 Paris Cedex 15, France. [7]Global Health Institute, Ecole Polytechnique Fédérale de Lausanne, CH-1015 Lausanne, Switzerland. [8]Inserm Avenir Group, Institut Pasteur Korea, 39-1 Hawolgok-dong, Seongbuk-gu, 136-791 Seoul, Korea. [9]Division of Cellular and Molecular Medicine, St. George's Hospital, University of London, Cranmer Terrace, SW17 ORE London, UK. [10]Statens Serum Institut, Department of Infectious Disease Immunology, Artillerivej 5, DK-2300 Copenhagen S, Denmark. [11]AstraZeneca India, Bellary Road Hebbal, Bangalore, India. [12]Center for Tuberculosis Research, Johns Hopkins University School of Medicine, Baltimore, MD 21231, USA.

*These authors contributed equally to this work.
†To whom correspondence should be addressed. E-mail: stewart.cole@epfl.ch

ERRATUM

Post date 5 June 2009

Reports: "Human induced pluripotent stem cells free of vector and transgene sequences" by J. Yu *et al.* (8 May, p. 797). Karyotypes were performed on each of the vector-free iPS cell clones analyzed and were reported to be normal. Through subsequent high-resolution chromosomal analysis by comparative genomic hybridization, a small interstitial deletion of chromosome 15 was identified in one of the clones (iPS-DF6-9-12T). Re-review of the original karyotypes revealed that this small deletion was present and missed, and that the initial karyotype depicted in Fig. 3B was not normal, but should have been reported as: 46,XY,del(15)(q14q15). The karyotypes for the other vector-free iPS cell clones analyzed were also re-reviewed, and all are apparently normal. The revised karyotype for clone iPS-DF6-9-12T does not change the substance of the paper given that the karyotypes of the remaining vector-free clones appear normal.